Influence of the Chromium Content on the Characteristics of the Matrix, the Tantalum Carbides Population, and the Hardness of Cast Co(Cr)-0.4C-6Ta Alloys

Patrice Berthod, Merzouk Bouaraba, Junfu Cai

micro

MDPI

Article

Influence of the Chromium Content on the Characteristics of the Matrix, the Tantalum Carbides Population, and the Hardness of Cast Co(Cr)-0.4C-6Ta Alloys

Patrice Berthod [1,2,*], Merzouk Bouaraba [2] and Junfu Cai [2]

[1] Institut Jean Lamour, CNRS, 2 Allée André Guinier, Campus Artem, 54000 Nancy, France
[2] Faculté des Sciences et Technologies, Université de Lorraine, Campus Victor Grignard, 54500 Vandoeuvre-lès-Nancy, France
* Correspondence: patrice.berthod@univ-lorraine.fr; Tel.: +33-372742729

Abstract: The mechanical and chemical behaviors of cast cobalt-base superalloys are governed by the carbides and by a reactive element, which is often chromium. The content of this later element, which is efficient in resisting hot oxidation and also hot corrosion, may have consequences on the melting temperature, microstructure, and mechanical properties at high temperatures and at room temperature. Seemingly, the effect of chromium content on the microstructure and properties of cast equi-axed Co-Cr-Ta-C superalloys containing TaC as single reinforcing carbide and in high-enough quantities to achieve a high level of creep resistance has not been the subject of previous investigations. The present work is devoted to the exploration of this influence of Cr content on the as-cast microstructure of a model alloy in this category, as well as on its microstructure transformations at high temperatures. The work aims to help rate the Cr content to achieve the best characteristics in machinability and high-temperature properties. This is of great importance for fabricability (production cost) and sustainability in service (long enough lifetime performance). A series of six alloys derived from a rather well-known alloy and presenting various Cr contents were thus elaborated by casting. Their microstructures were investigated in their as-cast state as well as in an aged state resulting from a 4-day stage at 1400 K. Vickers indentation was also carried out to study how hardness may evolve with Cr content. It was seen that the higher the Cr content, the lower the solidus temperature, the coarser the TaC population, the harder the alloy, and the higher the risk of brittleness. In order to reach the best compromise, the preferred Cr weight content range, as identified by this work, is 20–30%; indeed, for such Cr contents: (1) the matrix is austenitic, then dense, and then hard and not brittle, and thus is mechanically resistant and tough; (2) the TaC carbides are script-shaped and resistant against morphology changes at high temperatures, and thus efficiently preserve interdendritic cohesion for a long time, and, consequently, (3) the alloys are machinable, have expected good toughness, and can be resistant against creep deformation as well as oxidation and corrosion at high temperatures thanks to the Cr content, allowing for chromium-forming behavior.

Keywords: cobalt alloys; tantalum carbides; chromium content; as-cast microstructure; aged microstructures; hardness

Citation: Berthod, P.; Bouaraba, M.; Cai, J. Influence of the Chromium Content on the Characteristics of the Matrix, the Tantalum Carbides Population, and the Hardness of Cast Co(Cr)-0.4C-6Ta Alloys. *Micro* **2023**, *3*, 239–255. https://doi.org/10.3390/micro3010017

Academic Editor: Carlo Santulli

Received: 30 December 2022
Revised: 14 February 2023
Accepted: 14 February 2023
Published: 16 February 2023

1. Introduction

Industry, power generation, or transportation are sectors in which high temperatures may be encountered. Hot glass-making tools and the hottest parts of turbines and incinerators require materials that are high enough in toughness and resistance against mechanical stresses and the chemically aggressive worked melts and gases. The metallic materials that are the most extensively used to respond to these needs are superalloys. Not the best, but certainly one of the most universal superalloys, is the polycrystalline equi-axed coarse-grained cobalt superalloy, strengthened by carbides and rich in chromium, which has been available for a long time [1]. More recently, modern cobalt alloys with

strengthening mechanisms involving intermetallics have appeared [2]. Some Co-based superalloys that are strengthened by carbides contain only chromium carbides [3], such as the well-known X40 [4], or simultaneous chromium and tantalum carbides, such as the Mar-M509 superalloy [5]. It is also possible that TaC or other MC carbides (HfC, ZrC, etc.) are the single carbides in the same cobalt-based alloy [6]. In such a situation, very interesting mechanical properties at elevated temperatures can be obtained [7].

Recently, the formation of TaC was also promoted in a high-entropy alloy [8] based on Cantor's composition (equimolar CoNiFeMnCr). The presence of TaC resulted in very interesting creep resistance, even at 1100 °C [9].

Mar-M509 and the other alloys cited above are more or less rich in chromium. Their C content allows them to resist oxidation by hot gases and corrosion in melts such as glasses, sulfates, or CMAS. Tantalum and chromium are two carbide-forming elements (as seen again in the preceding words) that are in competition with one another. In contrast to nickel-based alloys, for which this competition is rather equilibrated and may lead to the coexistence of chromium carbides and tantalum carbides [10], tantalum carbides tend to remain stable and to stay as the single carbide phase that is present in Co-based alloys. However, for fixed contents of carbon and tantalum, increasing Cr beyond the usual 30 wt.% content value can intensify the corrosion resistance, especially in the case of an aggressive gaseous or molten milieu. But such Cr enrichment can also lead to the appearance of chromium carbides beside TaC. A consequence of that is a possible decrease in refractoriness. Inversely, in the case of quasi-absent corrosion risk, it can be interesting to lower the Cr content bellow 20 wt.% and even 10 wt.% to lower the production cost by using less chromium and by facilitating the foundry process.

Polycrystalline equi-axed cobalt-based superalloys containing interdendritic eutectic TaC carbides as the exclusive strengthening particles for resisting creep at high temperatures have not really been considered or studied around the world. Except for the ones concerning the directionally solidified Co(Cr)-based TaC(fibers)-strengthened superalloys developed several decades ago [11,12], or some recent works carried out by us (i.e., [6,8,9]), studies on such alloys consisting of a Co-(Cr) matrix and an interdendritic network of coarse eutectic TaC, are rare, and maybe nonexistent. Furthermore, logically, no works dealing with the influence of the chromium content on the characteristics of the matrix and of the carbides population seem to have been carried out, despite the fact that studies on the influence of Cr content in other types of Co alloys with TaC have been reported (e.g., Co-Re alloys with nano-sized TaC [13]).

For such TaC-strengthened polycrystalline cast cobalt-based superalloys, rating the chromium content at values significantly higher or significantly lower than the usual 30 wt.% content to obtain some of the benefits of different ways (for instance, better sustainability by improved high-temperature corrosion resistance, or lower production costs) of production without encountering prejudicial consequences (on microstructure, mechanical behavior, etc.) may be easier with good knowledge of the possible effect of such changes in the Cr content. The aim of this work is precisely to bring first responses by exploring and testing significant changes in chromium content in the compositions of cast(0.4C and 6Ta, wt.%)-containing cobalt-based alloys. Here, the explored effects concern microstructures, refractoriness, and hardness in order to give information by the identification of the best Cr content to achieve an interesting set of properties (fabrication, performance, and extended lifetimes).

2. Materials and Methods

2.1. Design of the Alloys for the Study

The reference alloy of this work is a Co(bal.)-30Cr-0.4C-6Ta. This is a simplified version of an industrial superalloy particularly used in the glass industry. From the 30 wt.%Cr present in this alloy, two lower contents (20 and 10 wt.%, and Cr-free alloy) and two higher contents (40 and 50 wt.%) were considered. All alloys were elaborated following the same

procedure, and the pure elements used to prepare the charges to melt came from the same source (Alfa Aesar, more than 99.9 wt.%).

2.2. Elaboration Details

The six 40 g charges were prepared with accuracy using a precision balance. All masses are given in Table 1. In this table, "00Cr", "10Cr", etc., are the designations of the different alloys, defined in relation to the weight percentage of chromium that they contain.

Table 1. Names of the six alloys and their weight contents in the different elements, with the corresponding masses for a 40 g ingot.

Total Weight: 40 g	**Co Contents and Masses**		**C Contents and Masses**		**Ta Contents and Masses**		**Cr Contents and Masses**	
00Cr	93.6 wt.%	37.44 g	0.4 wt.%	0.16 g	6 wt.%	2.4 g	0 wt.%	/
10Cr	83.6 wt.%	33.44 g	0.4 wt.%	0.16 g	6 wt.%	2.4 g	10 wt.%	4 g
20Cr	73.6 wt.%	29.44 g	0.4 wt.%	0.16 g	6 wt.%	2.4 g	20 wt.%	8 g
30Cr	63.6 wt.%	25.44 g	0.4 wt.%	0.16 g	6 wt.%	2.4 g	30 wt.%	12 g
40Cr	53.6 wt.%	21.44 g	0.4 wt.%	0.16 g	6 wt.%	2.4 g	40 wt.%	16 g
50Cr	43.6 wt.%	17.44 g	0.4 wt.%	0.16 g	6 wt.%	2.4 g	50 wt.%	20 g

The composed mixtures were each placed in the copper crucible of a high-frequency induction furnace (CELES, France), as illustrated in Figure 1. This crucible and the induction copper coil surrounding the crucible were both continuously cooled by the internal circulation of water. This cooling water was maintained at ambient temperature thanks to an external cooling apparatus. A silica tube was placed between the crucible (inner side) and the coil (outer side) to allow the closing of the fusion chamber, in which it was thus possible to manage the atmosphere. With several (pumping, followed by pure argon introduction) cycles, an internal atmosphere made of Ar at 300 mbars was created inside to prevent the possible oxidation of the elements during the high-temperature operations. Heating was induced (Foucault's currents) by a high-frequency alternative electric current (100 kHz, 5 kV of voltage). After the total melting of the charges, the temperature was maintained at its highest level for minimal duration (at least 10 min) to be sure to obtain a totally homogeneous liquid. Liquid-state cooling, solidification, and cooling-state cooling were produced by the regular decrease in injected power.

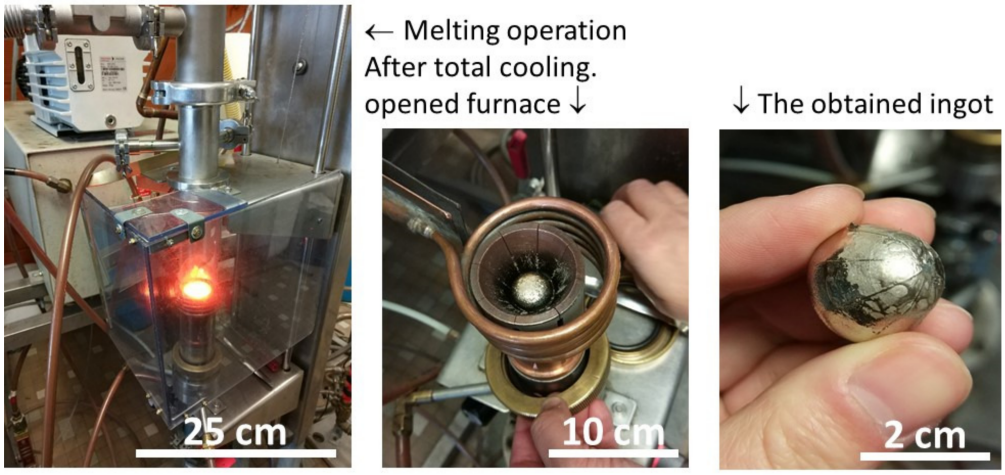

Figure 1. The melting alloy (**left**), the obtained ingot still in the crucible (**middle**), and after its extraction (**right**).

2.3. Sample Preparation, Exposure to High Temperatures, and Metallographic Characterization and Indentation

The ingots were cut with a metallographic saw in order to obtain the parts for the examination of the microstructures in the as-cast state and the samples for their exposure to high temperatures. The parts for preparing the metallographic samples were embedded in a mixture of resin and hardener, rigidifying at room temperature. They were thereafter ground (using SiC papers from #240 to #1200) and polished (using a textile disk enriched in micrometric hard particles).

The samples for high-temperature exposure were ground with #1200 SiC papers. Their edges were smoothed with the same SiC #1200 papers. They were placed in a resistive furnace where they were exposed to air at 1400 K (1127 °C) for 96 h (4 days). The aged samples were then prepared for metallographic observations, as already described above.

The as-cast and aged samples were all analyzed by energy dispersive spectrometry (EDS) to control the obtained chemical compositions (several full frame analyses at ×250) via the calculation of the average contents and of the corresponding standard deviation values. Microstructure observations were carried out with a scanning electron microscope (SEM, JEOL, model JSM6010LA, Tokyo, Japan) in Back Scattered Electrons (BSE) mode (acceleration voltage: 20 kV). The identification of the phases present (matrix, carbides) was carried out using EDS spot analysis. To quantitatively measure the surface fractions of the carbides, a series of ×1000 SEM/BSE micrographs were analyzed per sample using the image analysis tool included in the Photoshop CS software of Adobe (San José, CA, USA).

The hardness of each alloy for each of its two states of interest (as-cast and aged) was measured by Vickers indentation. Per sample, a series of indentations under 10 kg (load), were performed, followed by the calculation of the average and standard deviation values.

2.4. Thermodynamic Calculations

To help with the interpretation of the formation of the seen microstructures, thermodynamic calculations were performed using the Thermo-Calc (version N, Stockholm, Sweden) software, working with a suitable database. Isopleths were calculated to virtually reproduce the evolution of the alloys from the liquid state to the solid state at low temperatures. Individual calculations were carried out for each alloy for the 1400 K temperature.

3. Results and Discussion

3.1. Chemical Composition and Microstructures of the Alloys in Their As-Cast States

Prior to further work, the chemical compositions of the obtained alloys were controlled using the EDS spectrometer equipped with the SEM. A series of randomly selected ×250 areas were subjected to full frame analysis. The obtained results are given in Table 2. The Cr contents are very well respected. One can say that it is the same for Ta and C. Indeed, the tantalum contents were overestimated, as is classically found when EDS is performed on alloys in which a great part of the present tantalum exists as carbides. Indeed, these generally emerge in relief on the surface after final polishing due to having a hardness that is much higher than the matrix. Second, the obtained TaC population (as this will be seen soon thereafter) is typical of the 0.4% and 6% weight contents of similar alloys produced earlier with the same synthesis apparatus and following the same procedure in all details. For these earlier alloys, spark spectrometry, an efficient and accurate technique for most elements, including Ta and C, demonstrated that no carbon and no tantalum were lost during elaboration.

Table 2. The chemical compositions of the obtained alloys (several ×250 full-frame EDS analyses).

Alloy		00Cr	10Cr	20Cr	30Cr	40Cr	50Cr
Cr	AVERAGE CONTENT	/	10.26 wt.%	21.11 wt.%	30.60 wt.%	40.26 wt.%	50.06 wt.%
	Standard deviation	/	0.22 wt.%	0.18 wt.%	0.39 wt.%	0.14 wt.%	0.67 wt.%
Ta	AVERAGE CONTENT	6.86 wt.%	5.84 wt.%	7.18 wt.%	7.15 wt.%	6.77 wt.%	6.65 wt.%
	Standard deviation	0.04 wt.%	1.38 wt.%	0.68 wt.%	0.24 wt.%	0.18 wt.%	1.04 wt.%

The microstructures of these as-cast alloys were examined at various magnifications. Per alloy, two of these SEM/BSE micrographs were kept for their representativity, one (×250) for a general view of the microstructure, and one (×1000) to allow for a detailed examination. They are shown in Figure 2 for the 00Cr and 10Cr alloys, in Figure 3 for the 20Cr and 30Cr alloys, and in Figure 4 for the 40Cr and 50Cr alloys.

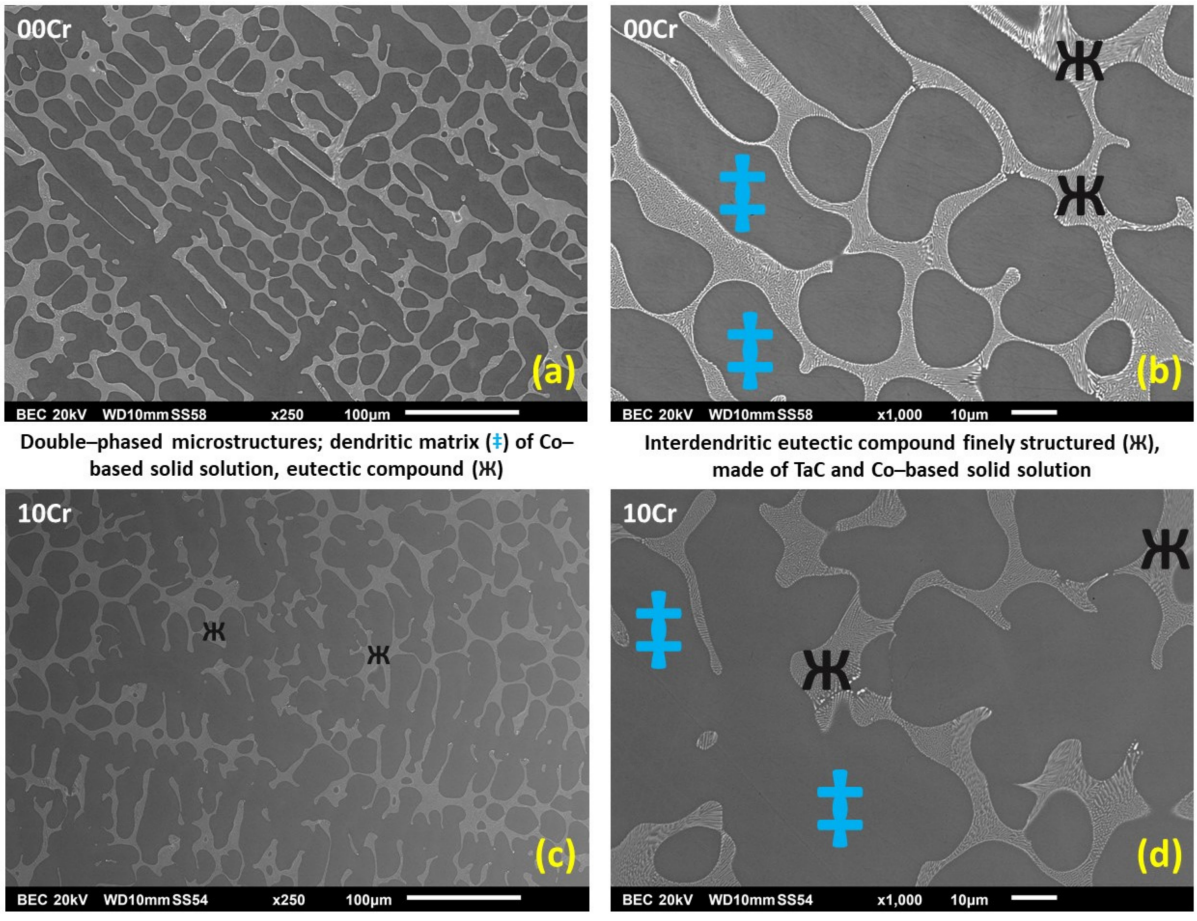

Figure 2. As-cast microstructures of the 00Cr (**a**,**b**) and 10Cr (**c**,**d**) alloys; general (×250: **a**,**c**) and detailed (×1000: **b**,**d**) views.

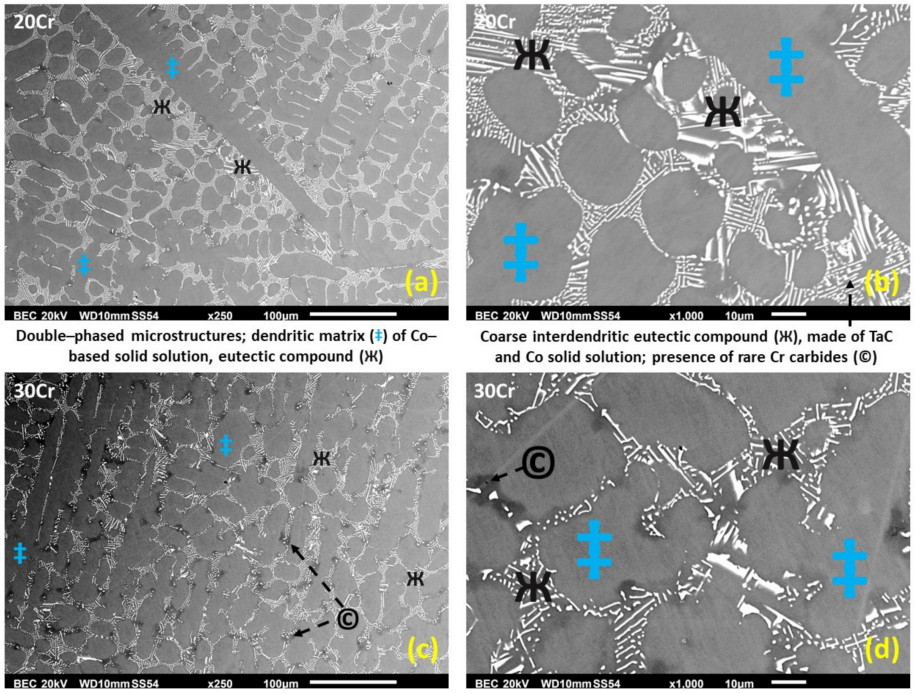

Figure 3. As-cast microstructures of the 20Cr (**a**,**b**) and 30Cr (**c**,**d**) alloys; general (×250, **a**,**c**) and detailed (×1000, **b**,**d**) views.

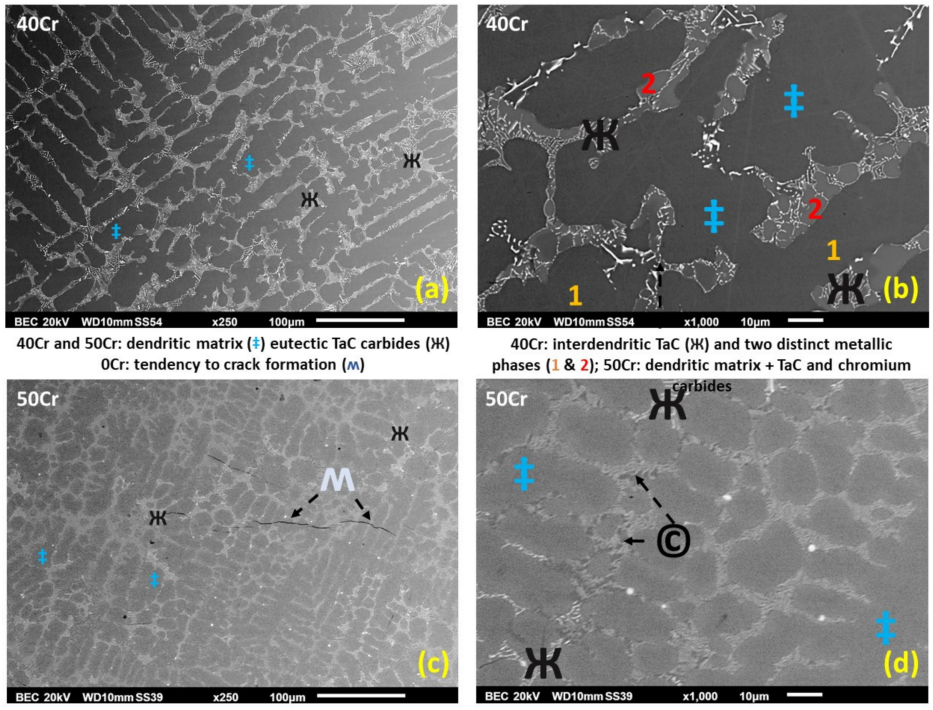

Figure 4. As-cast microstructures of the 40Cr (**a**) and 50Cr (**c**) alloys; general (×250: **a**,**c**) and detailed (×1000: **b**,**d**) views.

The four first alloys, from 00Cr to 30Cr, present microstructures that are rather similar to one another. These four microstructures are made of a dendritic matrix and of an interdendritic compound. The latter one is bright and finely structured in the cases of the 00Cr and 10Cr alloys and coarser in the cases of the 20Cr and 30Cr alloys, for which the metallic phase (same gray level as the dendritic matrix) and a bright script-like phase are much easier distinguish. The EDS spot analysis performed on the coarsest particles

indicates that these bright, script-like particles are tantalum monocarbides (TaC). EDS X-mapping was run to chemically illustrate the two types of TaC fineness. The results are shown in Figure 5 (00Cr alloy) and Figure 6 (30Cr alloy). In the later X-map, one can also observe that the darker zones visible here and there in the interdendritic areas are still the matrix, but this is enriched with segregated chromium.

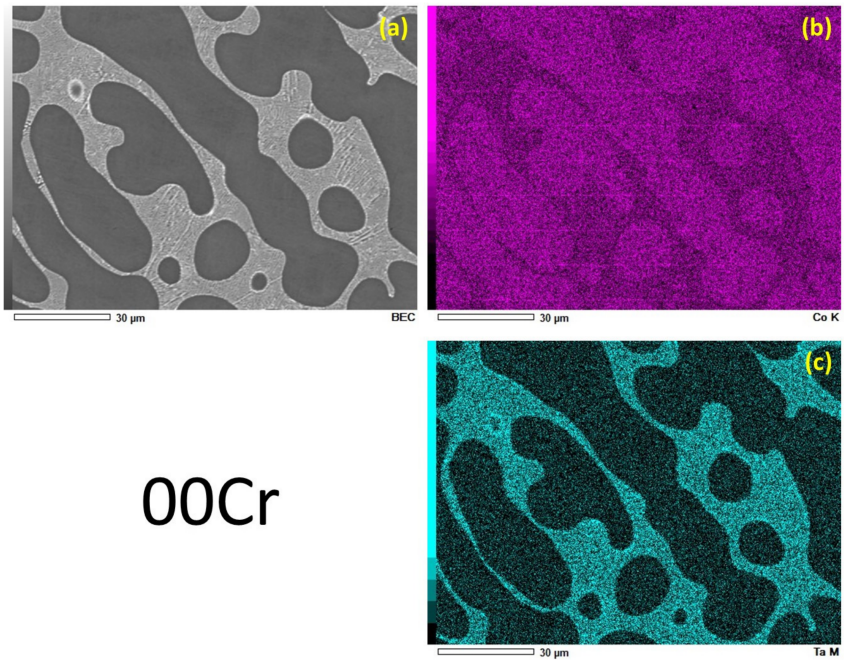

Figure 5. EDS X-cards (SEM/BSE: (**a**), Co: (**b**), Ta: (**c**)) illustrating the element repartitions in the microstructures of the two alloys with finely structured (matrix + TaC) eutectic compounds (here: the 00Cr alloy).

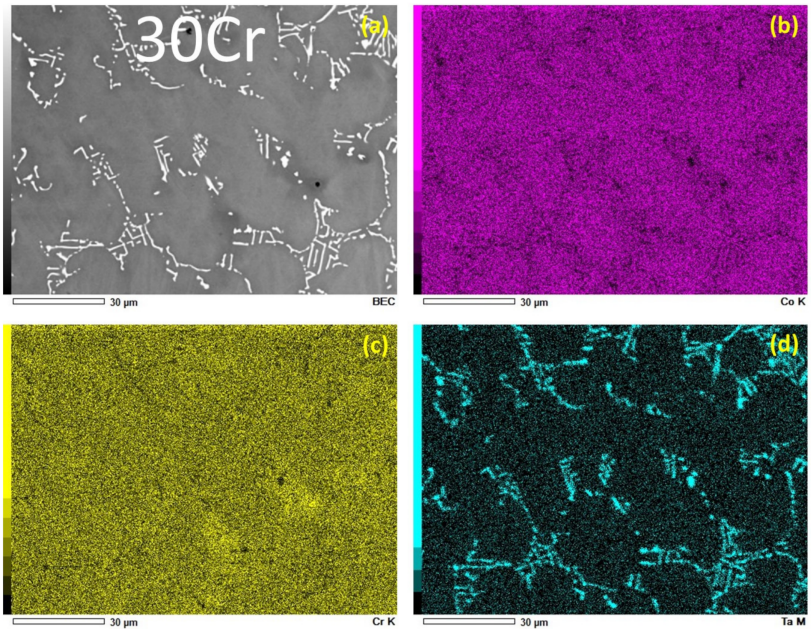

Figure 6. EDS X-cards (SEM/BSE: (**a**), Co: (**b**), Cr: (**c**), Ta: (**d**)) illustrating the element repartitions in the microstructures of the two alloys with finely structured (matrix + TaC) eutectic compounds (here the 30Cr alloy).

The 40Cr and 50Cr alloys are microstructurally different. In the first one, the particularity (by comparison to the 00Cr to 30Cr alloys) concerns the interdendritic phases. Despite its tendency to form a script-like shape, the TaC of the 40Cr alloy seems to be morphologically intermediate between the finely structured TaC of the 00Cr and 10Cr alloys and the coarser TaC of the 20Cr and 30Cr alloys. However, the main particularity is the metallic phase forming the eutectic with TaC: this one is paler than the matrix dendrites, and it also presents a well-defined border with the matrix.

The matrix of the 50Cr alloy is obviously similar to the pale metallic phase seen in the 40Cr alloy. One must also mention that the chromium carbides seem to have precipitated in the interdendritic areas next to the script-like TaC carbides.

Per alloy, a series of EDS spot analyses were performed on all the metallic phases seen in the microstructures (single dendritic matrix for the 00Cr, 10Cr, 20Cr, 30Cr and 50Cr alloys, dendritic matrix and eutectic metallic phases for the 40Cr alloy). Table 3 gives the results.

Table 3. Chemical compositions of the metallic phases present in the six alloys (all contents in wt.%).

Alloy		0Cr	10Cr	20Cr	30Cr	40Cr	50Cr
Cr	AVERAGE CONTENT	/	10.42 wt.%	20.32 wt.%	30.01 wt.%	m1 (38.77) m2 (46.61)	55.17 wt.%
	Standard deviation	/	0.26 wt.%	0.27 wt.%	0.19 wt.%	m1 (0.12) m2 (1.77)	1.24 wt.%
Ta	AVERAGE CONTENT	2.48 wt.%	2.59 wt.%	2.17 wt.%	2.30 wt.%	m1 (2.13) m2 (5.53)	1.52 wt.%
	Standard deviation	0.24 wt.%	0.76 wt.%	0.11 wt.%	0.29 wt.%	m1 (0.22) m2 (0.34)	0.37 wt.%

Unsurprisingly, chromium is concentrated in the matrix, in which the content is slightly higher than in the alloy itself. This is logical when one takes into account that Cr does not take part in the carbides and that the matrix volume is slightly smaller than the alloy volume. Concerning tantalum, the major part is involved in the TaC carbides, but about 2-2.5 w.%Ta is contained in the dendritic matrix. The second metallic phase existing in the 40Cr alloy (pale phase mixed with the script-like TaC) is about three times richer in Ta than in the dendritic matrix, which explains its slightly brighter gray in the SEM/BSE micrographs (higher average molar mass).

3.2. Microstructures of the Alloys after Aging at 1400 K

The samples from the six alloys were reheated at 1400 K for a long time in order to observe how their microstructures might evolve during service at such high temperatures. After having been exposed for 96 h (i.e., 4 whole days) at 1400 K (1127 °C), the obtained aged samples were prepared as metallographic samples and examined with the SEM in BSE mode. The illustrative micrographs are provided in Figure 7 (00Cr and 10Cr alloys), Figure 8 (20Cr and 30Cr alloys), and Figure 9 (40Cr and 50Cr alloys). In these figures, the aged microstructure is framed with an orange square, and a part of the micrograph of the as-cast version of the alloy is reminded on its left side to make it easy to compare the initial and aged microstructures.

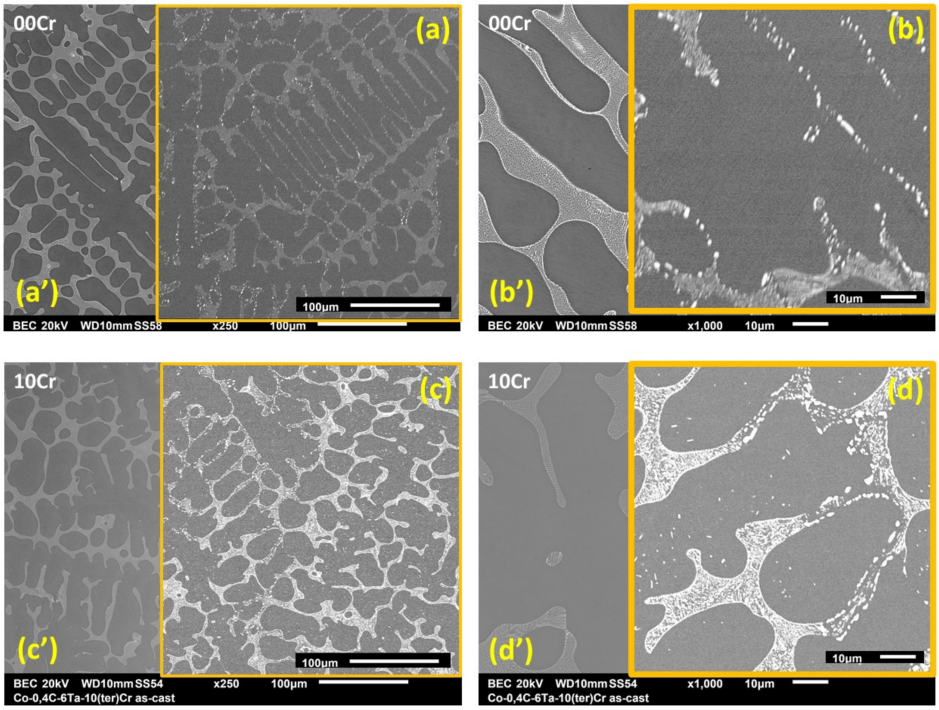

Figure 7. The (1400 K; 96 h)-aged microstructures (framed in orange) of the 00Cr (**a**,**b**) and 10Cr (**c**,**d**) alloys; general (×250: (**a**,**c**)) and detailed (×1000: (**b**,**d**)) views; addition of the as-cast microstructures (00Cr: (**a**′,**b**′), 10Cr: (**c**′,**d**′)) for comparison.

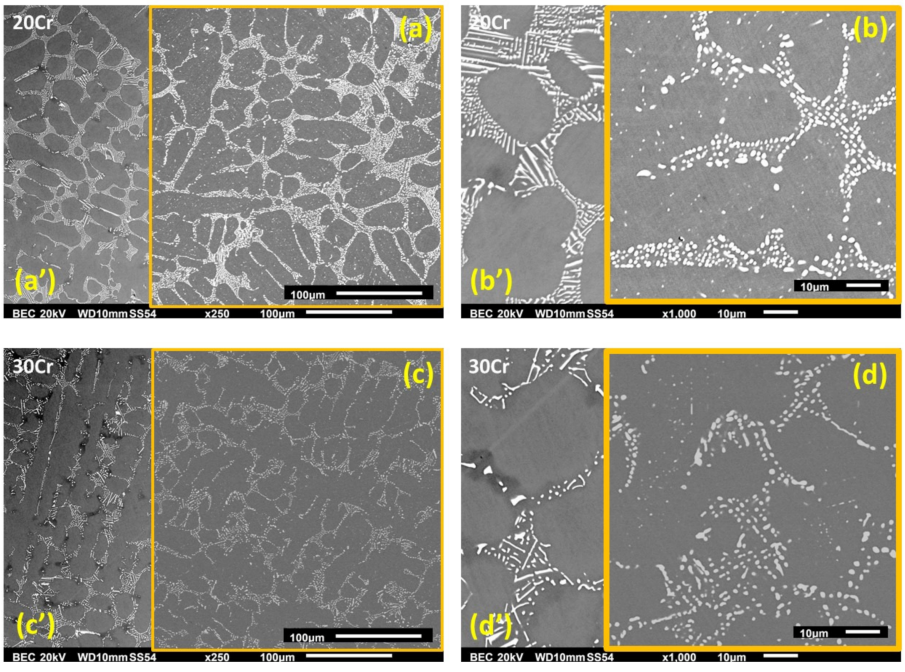

Figure 8. The (1400 K; 96 h)-aged microstructures (framed in orange) of the 20Cr (**a**,**b**) and 30Cr (**c**,**d**) alloys; general (×250: (**a**,**c**)) and detailed (×1000: (**b**,**d**)) views; addition of the as-cast microstructures (20Cr: (**a**′,**b**′), 30Cr: (**c**′,**d**′)) for comparison.

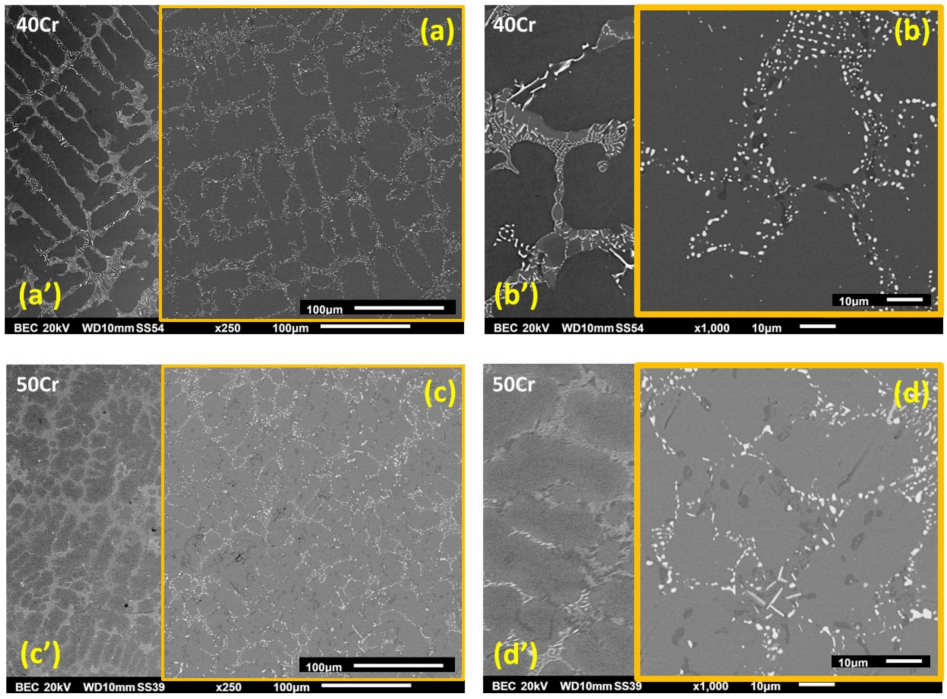

Figure 9. The (1400 K; 96 h)-aged microstructures (framed in orange) of the 40Cr (**a**,**b**) and 50Cr (**c**,**d**) alloys; general (×250: (**a**,**c**)) and detailed (×1000: (**b**,**d**)) views; addition of the as-cast microstructures (40Cr: (**a**′,**b**′), 50Cr: (**c**′,**d**′)) for comparison.

One can see that the TaC carbides evolved slightly during the high-temperature exposure, becoming a little fragmented and coalesced. This limited globularization phenomenon is promoted by the need for interfacial reduction from the free energy of the alloys, with all alloys tending towards better stabilization. This is similar to what takes place in pearlitic steels or cast irons, such as in the cementite lamellae present in pearlite when a heat treatment at close to 700 °C is applied: in these heat-treated pearlitic alloys, the Fe_3C lamellae are transformed into alignments of Fe_3C round particles. This well-known heat treatment, called pearlite globularization, aims to enhance both toughness and ductility.

In addition, one can see that fine secondary TaC carbides have precipitated in the matrix (in the cores of dendrite arms) and also that the chromium carbides have precipitated in the 40Cr and 50Cr alloys. The pale metallic phase, in which the script-like eutectic TaC was mixed into the interdendritic areas when 40Cr was in its as-cast state, has disappeared. It is possible that this solid-state transformation of this minor metallic part of the microstructure is responsible for the particularly great fragmentation of the TaC (by comparison with the other alloys). Such effects are seemingly not yet evocated and commented on in the existing literature. It merits further study with additional investigations.

The EDS spot analyses were performed again in the matrix of the alloys after aging. The results, displayed in Table 4, show that almost all chromium is still contained in the matrix. They also show that the Cr content in the aged 40Cr alloy is now closer to that initially contained in the dendritic matrix of the as-cast alloys (than to the metallic phase), which existed in the interdendritic spaces where it was next to TaC. A part of Ta (about the third part of the total tantalum) is in the matrix (the rest being in the form of TaC carbides).

Table 4. Chemical compositions of the matrixes of the aged alloys.

Alloy		0Cr	10Cr	20Cr	30Cr	40Cr	50Cr
Cr	AVERAGE CONTENT	/	10.60	21.94	31.92	39.41	51.21
	Standard deviation	/	0.12	0.48	0.90	2.04	1.19
Ta	AVERAGE CONTENT	2.47	2.51	1.37	1.60	3.91	2.89
	Standard deviation	0.72	0.68	0.11	0.12	3.76	0.74

3.3. Interpretation of the As-Cast States and Aged States Using Thermodynamic Calculations

The high-temperature part of a (0.4wt%C, 6wt.%Ta) isopleth computed with Thermo-Calc is given in Figure 10. It allows for an understanding of how the microstructures formed during solidification. From the liquid state, the 00Cr, 10Cr, 20Cr, and 30Cr alloys started their solidifications with nucleation and then the growth of the Co-based "face-centered cubic" (FCC) solid solution, which developed as dendrites. The solidification of the 50Cr alloy also began with the development of dendrites, but these ones are made of a "body-centered cubic" (BCC) network. For these five alloys, solidification was finished by a final (residual liquid → matrix + TaC) eutectic reaction. During the high-temperature part of the solid-state cooling (down to 1500 K), the four first alloys were still double-phased (FCC matrix + TaC), while the 50Cr alloys encountered further solid-state transformations before reaching 1500 K. These solid-state transformations represent the precipitation of $Cr_{23}C_6$ carbides next to the TaC and the transformation of the BCC matrix in a mixture of FCC and the sigma phase (peritectic reaction). The behavior of the 40Cr alloy during solidification was intermediate between the 30Cr and the 50Cr alloys.

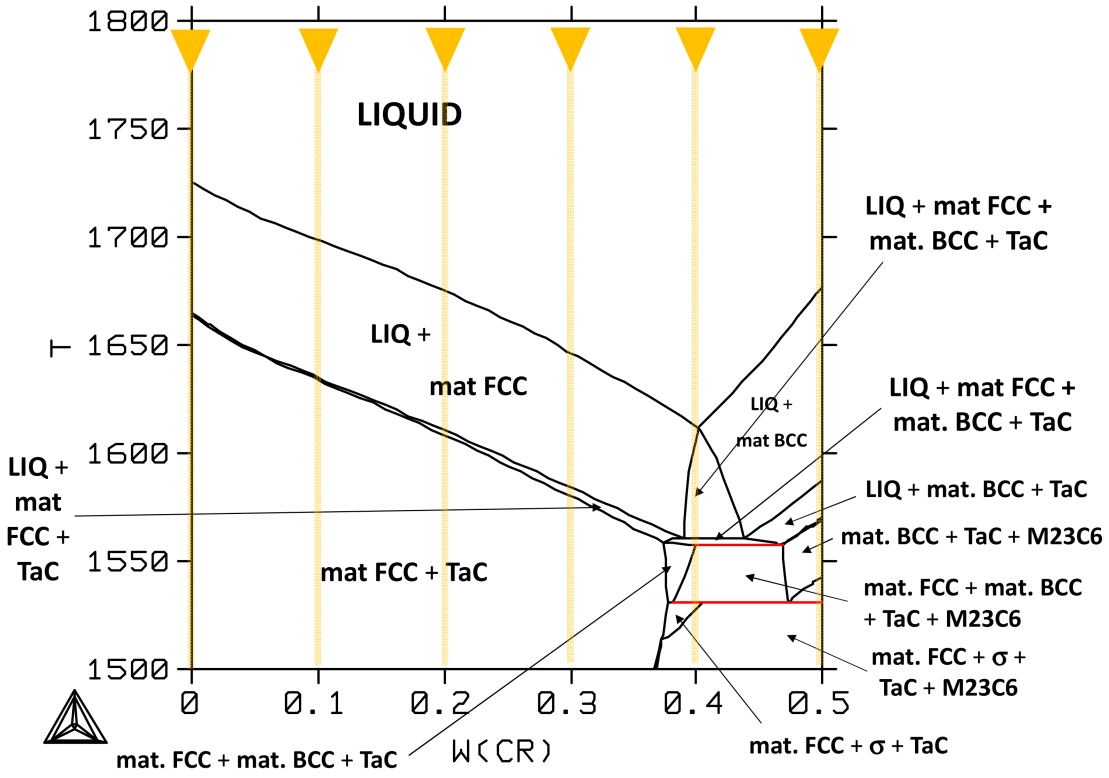

Figure 10. High-temperature part of a (0.4wt%C, 6wt.%Ta) isopleth, computed with Thermo-Calc (the six alloys are materialized by orange triangles followed by vertical lines).

Figure 10 is completed by Figure 11, which presents the same isopleth section but for medium temperatures between 1500 and 1200 K. This second part of the isopleth section allows us to see that, if one can consider that further solid-state transformations are not kinetically possible under 1200 K (923 °C) for such refractory metallurgical systems, the following solid-state cooling did not induce qualitative changes in the (FCC matrix + TaC) microstructures of the 00Cr, 10Cr, and 20Cr alloys: this is confirmed by what was observed in these alloys in their as-cast states. According to the isopleth section, at 1200 K, the 40Cr and 50Cr alloys are expected to contain $Cr_{23}C_6$ carbides in addition to the TaC. This is what was observed, yet in rather small quantities (dark particles in Figure 9). Concerning the matrixes, according to Thermo-Calc, the high-temperature FCC version of the 30Cr alloy was expected to be partly converted into HCP, and in the final versions of the 40Cr and 50Cr alloys, a mixture of hexagonal close-packed (HCP) and of sigma-phase (CoCr type), and of sigma-phase only, respectively.

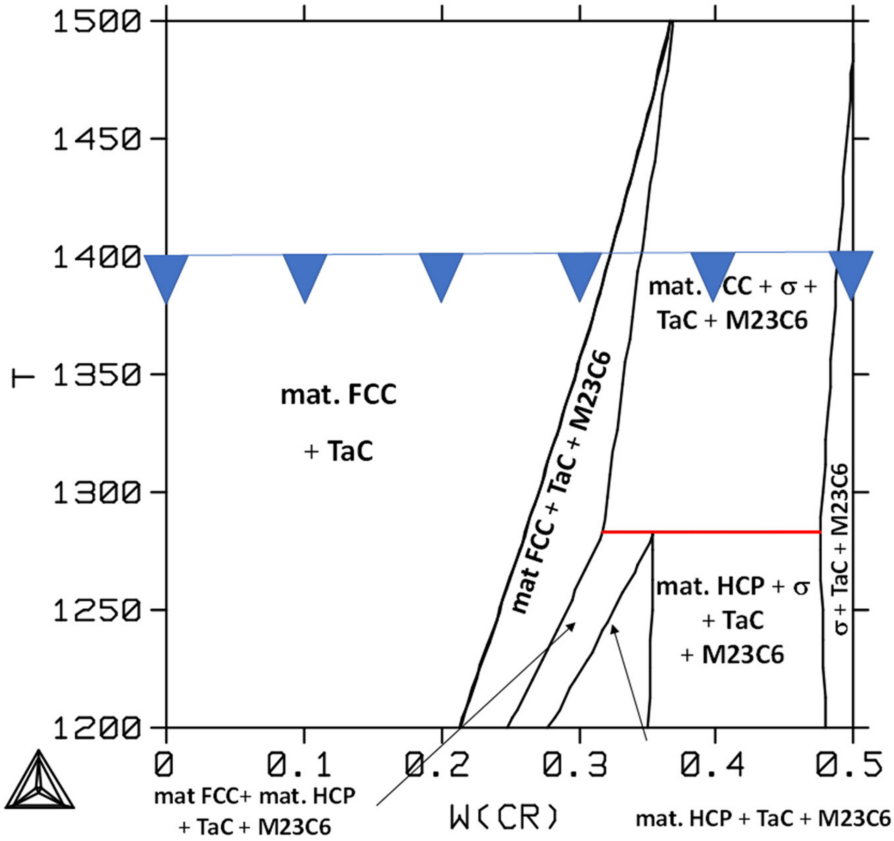

Figure 11. Medium temperature part of a (0.4wt%C, 6wt.%Ta) isopleth, computed with Thermo-Calc (the position of the six alloys at the aging treatment temperature are materialized by blue triangles).

According to thermodynamic calculations, at 1400 K, aging is expected to allow the 00Cr, 10Cr, 20Cr, and 30Cr alloys to reach a stable state composed of the FCC Co-based solid solution matrix and the TaC carbides. These calculations are seemingly consistent with the obtained microstructures (Figures 7 and 8). Good agreement is also found between the calculated predictions and the aged microstructures of the 40Cr and 50Cr alloys (Figure 9): co-existence of TaC and chromium carbides ($Cr_{23}C_6$).

3.4. Comparison of Thermodynamic Calculations and Metallographic Observations

Image analysis was carried out on a series of ×1000 SEM/BSE micrographs per alloy to estimate the TaC surface fractions in the as-cast and aged conditions. The only phase that was really possible to consider was the TaC carbide phase, the bright gray of which was far enough from the matrix and chromium carbide gray levels. The results are graphically

presented, with the calculated results (calculated mass fractions converted into volume fractions, then into surface fractions using the volume masses of the matrixes and of the two types of carbides) in Figure 12.

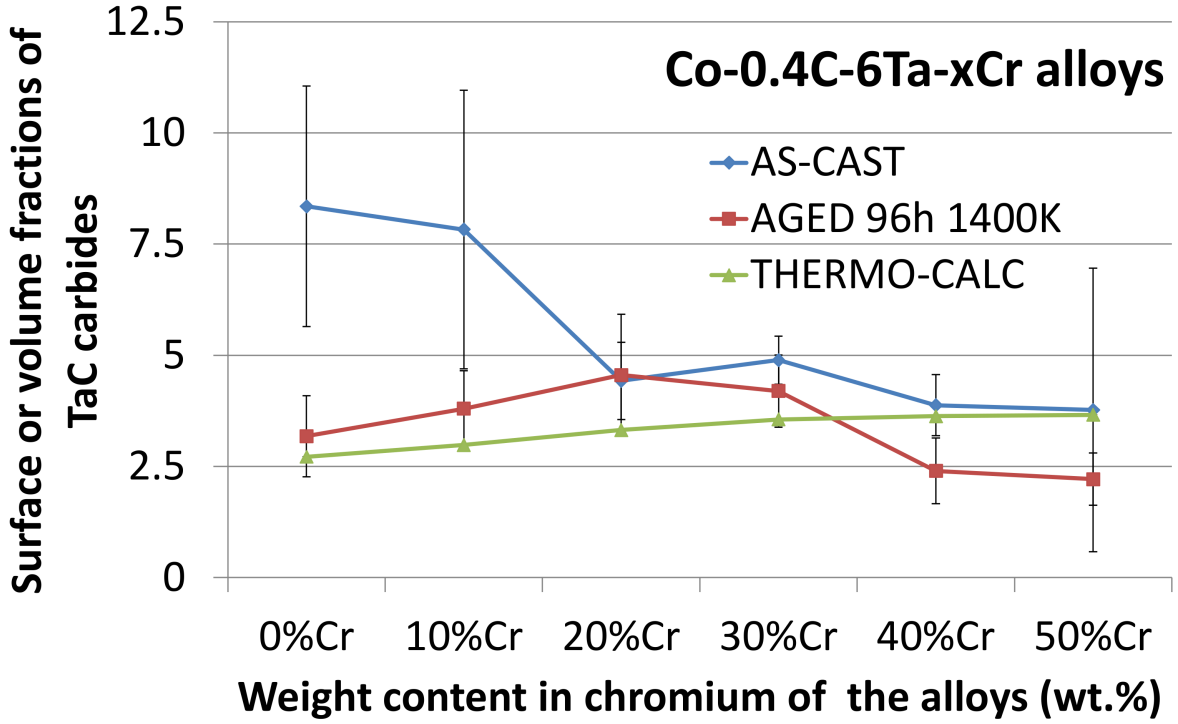

Figure 12. Evolution of the measured or predicted surface volume fraction in TaC versus the chromium content in the alloy.

In the as-cast state, the image analysis led to results showing that there the alloys with the two lowest Cr contents (00Cr and 10Cr) were the richest in TaC carbides. This observation, which is in total disagreement with both the image analysis results from the aged alloys and with thermodynamic calculation, is easily explainable by the particular fineness of the eutectic compounds in which the TaC carbides take part. This very fine eutectic maximized the influence of the TaC carbides on the brightness of these zones (participation of subjacent TaC). After aging at 1400 K, the same alloys were considered (by image analysis) to contain much more moderate TaC in terms of surface fraction, thanks to TaC fragmentation and coalescence, which gives more visibility to the second phase present in these eutectic areas matrix. This remarkable fineness of the (TaC, FCC matrix) interdendritic areas is possibly due to the high rate of cooling due to the particularly high liquidus temperatures of the 00Cr and 10Cr alloys (about 1725 K and 1700 K for 00Cr and 10Cr, respectively, Figure 10). Indeed, at such high temperatures, cooling was certainly fast, and this may have possibly promoted significant undercooling, with as consequences a fast eutectic solidification, and therefore the great fineness of the formed eutectic compound. Except for the values of TaC fraction in the as-cast states of the 00Cr and 10Cr alloys, the as-cast state, aged state, and theoretical TaC surface or volume fractions are rather consistent with one another. The TaC fraction values corresponding to the 00Cr to 30Cr alloys after aging tend to be slightly higher than the calculated ones, but they become lower than the calculated ones for the 40Cr and 50Cr alloys. This is the probable consequence of the formation of chromium carbides at the expense of some TaC, which was observed in the aged alloys: For these two alloys, Thermo-Calc did predict the presence of $Cr_{23}C_6$ carbides but in much lower quantities than what was really observed in the aged 40Cr and 50Cr alloys.

3.5. Indentation Results

Per alloy and for both states (as-cast and aged), a series of Vickers indentations under a 10 kg load were carried out. The results are given as graphs in Figure 13. From the 00Cr alloy to the 50Cr alloy, the Vickers hardness continuously increases, with a rough acceleration when reaching the 40Cr alloy, and even more for the 50Cr alloy. The progressive increase from 00Cr to 30Cr can be attributed to both the slight increase in TaC fraction (Figure 12) and the Cr-enrichment of the Co-based matrix by solid solution strengthening. The more marked increase in hardness from 30Cr to 40Cr, and especially to 50Cr, are certainly due to the partial replacement of the ductile austenitic matrix by the harder HCP Co-based phase and by the hard and brittle Co-Cr sigma phase favorable to its brittle rupture behavior (Figure 14).

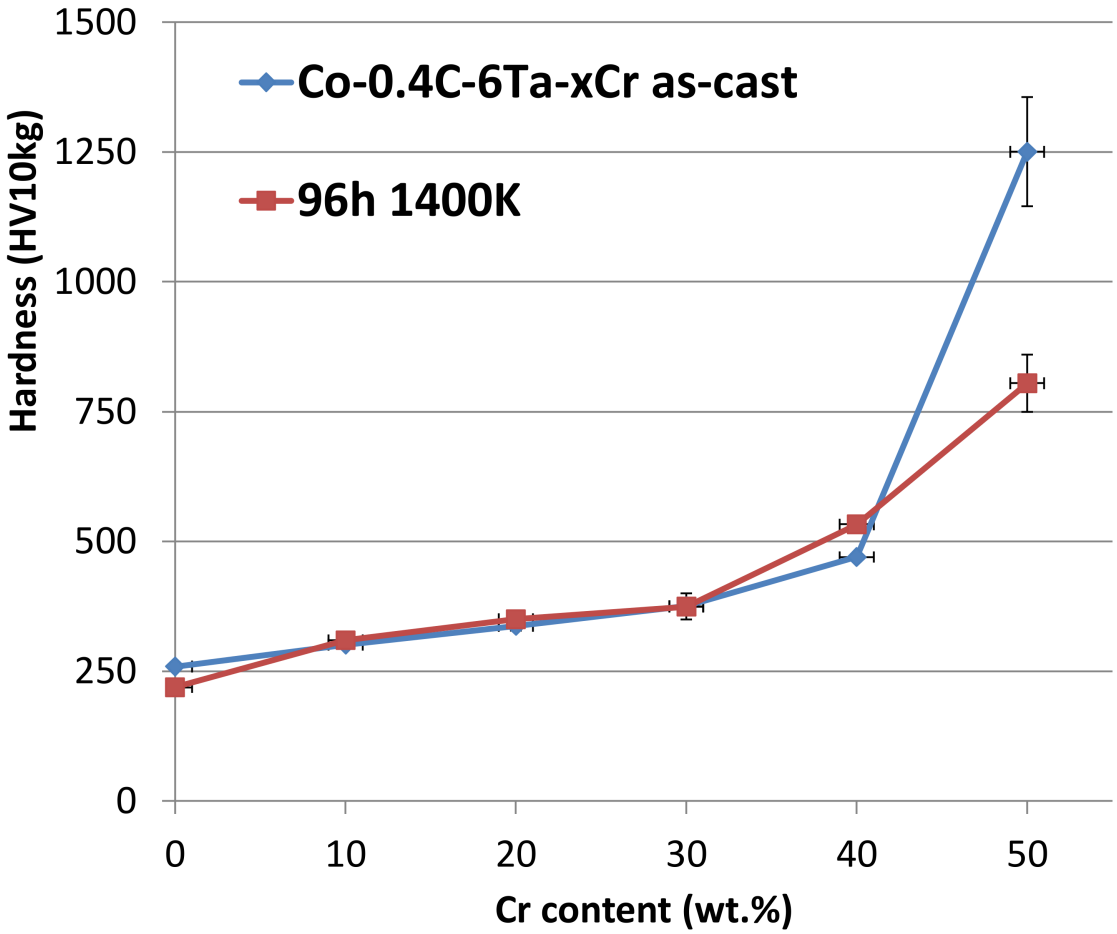

Figure 13. Hardness of the six alloys in their as-cast states and aged states, plotted versus the chromium content in the alloy (Vickers method, load: 10 kg).

3.6. Discussion

The first effect of the chromium content which was evidenced here concerns the matrix of the alloys. This one is dendritic in all cases, what is due to their chemical compositions. First, for the fixed contents in C and Ta, whatever the Cr content between 0 and 50 wt.% (and the resulting Co contents), the decrease in temperature from the total liquid state obviously leads, in the quaternary phase diagram, to the contact with the crystallization surface of the FCC Co-based or BCC Cr-based solid solution (FCC at low Cr and high Co in the alloy; BCC at very high Cr and low Co in the alloy). The matrix is, thus, in all cases, the first solid crystalline phase to appear. This metallographic result is confirmed by the visualization of the isopleth sections computed using Thermo-Calc. Further, due to the

well-known undercooling phenomenon, which usually appears because of the rejection of the solute atoms resulting from a fall in solubility accompanying the liquid → solid phase transformation, the solid–liquid interfacial instabilities appear and become more and more amplified [14]. This causes dendritic formation in the matrix for the forming alloys, and, as consequence, a high degree of continuity (over millimetric distances) of this resistant and tough metallic phase, with great interdendrites imbrication. These characteristics of the matrix, which are interesting for the future properties of the alloys in the mechanical field (and especially at high temperature), are preserved no matter what the change in Cr content (in the concentration range considered here).

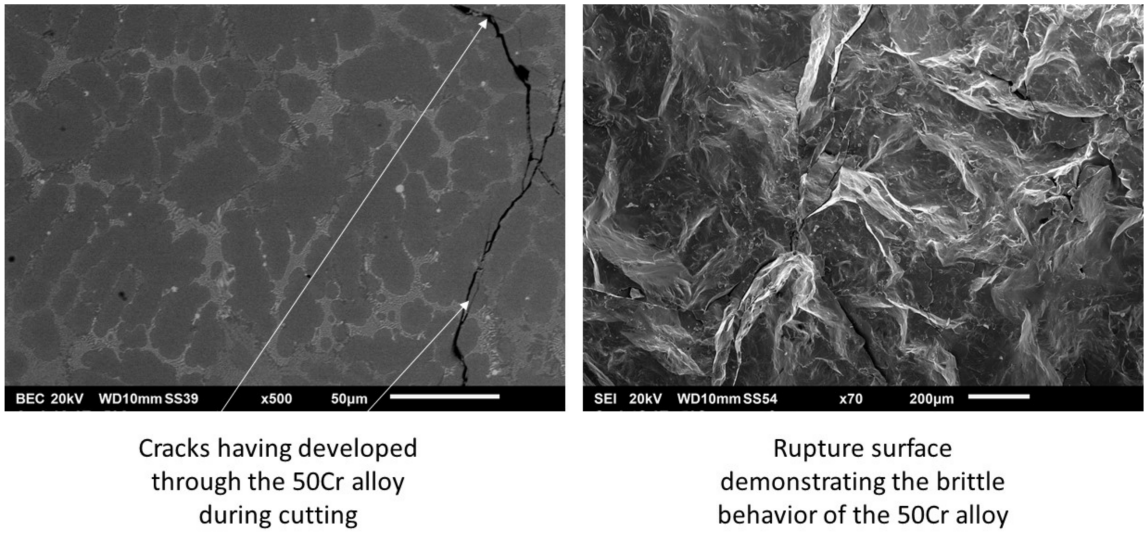

Figure 14. Crack propagation in the 50Cr alloy during cutting and fractographic view of a broken ingot.

Concerning the as-cast microstructures, a second point concerns the tantalum carbides. In the absence of chromium or for 10 wt.%Cr in the alloy, the interdendritic compound is very finely structured in comparison to the coarser structures of the eutectic (matrix + TaC) compound obtained for 20 or 30 wt.%Cr. The coarse eutectic is commonly found in cast polycrystalline equi-axed 30 wt.%Cr-containing Co-based superalloys, in which TaC is present together with other carbides [15], or in which TaC is the single carbide phase present [16]. The origins of the very fine eutectic can be the fast solidification of the (matrix + TaC) eutectic compound at the end of the solidification of the alloys free from chromium or containing little Cr in comparison to the alloys containing 20 or 30 wt.%Cr. Indeed, with several tens of Celsius degrees less than the 00Cr and 10Cr, the 20Cr and 30Cr cooled at a lower rate when the eutectic reaction took place due to the general hyperbolic type of the cooling curves. It is effectively well-known that slow cooling leads to cast microstructures that are coarser than the ones developed at high cooling rates [17]. Concerning the as-cast microstructure of the 40Cr alloy, it is characterized by the presence of a Cr-rich BCC phase in the interdendritic spaces, which is thereafter transformed into a CoCr sigma phase during postsolidification solid-state cooling. During FCC matrix growth, the segregation of the alloying elements—notably of Cr—is certainly at the origin of the crystallization of a Cr-rich BCC phase in the last zones to solidify. The constant rejection of Cr by liquid becoming the dendritic FCC solid solution led to the Cr enrichment of the liquid and, consequently, to the formation of the Cr-rich BCC phase. In the same location, TaC, which coprecipitated with the Cr-rich BCC phase at the end of solidification, presents fine morphology. Such a fine TaC microstructure is logically observed in the as-cast microstructure of the 50Cr alloy; indeed, due to the high Cr content in this alloy, solidification started with the crystallization of a BCC Cr-rich phase and finished with the coprecipitation of the BCC Cr-rich phase and TaC carbides. One must notice the presence

of some chromium carbides, the formation of which was favored by the high Cr content of the alloy (Thermo Calc isopleth).

After aging at 1400 K for 96 h, the thermodynamic stable state was established at the expense of the initial nonequilibrium microstructure formed during cooling. The chemical homogenization (notably, with the deletion of the segregations developed during solidification) allowed for the suppression of the Cr-enriched interdendritic zones (including the interdendritic BCC phase in the 40Cr alloy). A part of the interdendritic TaC precipitated (in great quantities) at the end of solidification was dissolved, consequently, to the Ta homogenization with the dendrites cores. In addition, the tendency to decrease the interfacial energy associated with the interphase surfaces separating the matrix and carbides naturally led to the loss of the elongated shapes of the TaC for the benefit of globular TaC. The fragmentation and coarsening of the TaC phase affected all alloys. At the same time, fine globular TaC nucleated and precipitated in the core of the dendrites. This obtained solid-state secondary precipitation brought TaC particles, which can be useful for the resistance against creep since they act as obstacles to dislocation movement in the case of applied stresses at high temperatures.

The fragmentation of the TaC induced a small decrease in hardness for all alloys due to the lack of continuity of the hard carbide interdendritic network. However, hardness stayed high (more than 500 Hv) for the 40Cr alloy, the matrix of which is HCP. The hardest alloy is 50Cr, with more than 750 Hv. This high hardness is due to the CoCr sigma phase constituting its matrix, which elsewhere lowered its ductility and toughness, as demonstrated by the presence of multiple cracks. Clearly, such high Cr contents are to be avoided, even if high levels of chromium may be required in critical, hot corrosion problems in service (work in highly aggressive milieus). Surface and subsurface chromium enrichments, produced by the pack cementation process [18,19], for instance, can afford such high corrosion resistance without the loss of the necessary ductility and toughness at low and high temperatures.

4. Conclusions

The chromium content influences the microstructure and the mechanical properties of the Co-0.4C-6Ta base alloy. For low Cr contents, the solidus temperature is particularly high, which is favorable for high-temperature mechanical resistance, but, unfortunately, the script-like shape of the eutectic TaC, which is good too for creep resistance, can be replaced by less favorable morphology. Regarding Cr contents that are too high, the matrix can be partly made of a hard HCP solid solution or by a brittle sigma phase. Such sigma phases may threaten machinability, ductility, and toughness at room and high temperatures. 30 wt.%Cr, already known for being favorable in high-temperature resistance against oxidation and corrosion, is thus to be preferred since it allows a reliable austenitic matrix to be kept, with good characteristics for the eutectic tantalum carbides (script-like closely mixed with the dendrites periphery). However, 20 wt.%Cr still maintains our interest since all the advantages of the Co-0.4C-6Ta-30Cr are kept, with an additional higher solidus temperature (favorable to higher creep resistance), but without the good high-temperature chemical resistance of 30 wt.%. Nevertheless, surface and subsurface Cr-enrichment by the pack cementation process, followed by diffusion heat treatment, can be considered for Co-0.4C-6Ta-20Cr alloys so as to contain about 30 wt.%Cr in its outermost part for good oxidation and corrosion resistance.

The observations of this work are summarized as follows:

- Decreasing the Cr content down to 10 wt.% refines the eutectic TaC;
- 20 to 30 wt.%Cr keeps the script-like shaped TaC, which is known to be favorable against creep resistance;
- Cr contents beyond 40 wt.% decrease TaC stability and favor the minor presence of chromium carbides;
- Cr contents beyond 40 wt.% induce matrix changes from FCC to HCP, and the CoCr sigma phase enhances hardness and brittleness and decreases toughness;

- A Cr content close to 30 wt.% is best for good general high-temperature behavior.

5. Patents

There are no patents resulting from the work reported in this manuscript.

Author Contributions: Conceptualization, P.B.; methodology, P.B.; software, P.B.; validation, P.B.; formal analysis, P.B., M.B. and J.C.; investigation, P.B., M.B. and J.C.; resources, P.B.; data curation, P.B.; writing—original draft preparation, P.B.; writing—review and editing, P.B.; visualization, P.B.; supervision, P.B.; project administration, P.B. All authors have read and agreed to the published version of the manuscript.

Funding: This research received no external funding.

Institutional Review Board Statement: Not applicable.

Informed Consent Statement: Not applicable.

Data Availability Statement: Not applicable.

Conflicts of Interest: The authors declare no conflict of interest.

References

1. Sims, C.T.; Hagel, W.C. *The Superalloys*; John Wiley & Sons: New York, NY, USA, 1972.
2. Tang, C.; Pan, F.; Qu, X.; Duan, B.; Wang, T.; He, X. Novel cobalt base superalloy and its high-temperature flow behavior. *Rare Met.* **2008**, *27*, 292–298. [CrossRef]
3. Jiang, W.H.; Yao, X.D.; Guan, H.R.; Hu, Z.Q. Relationship between degeneration of M_7C_3 and precipitation of $M_{23}C_6$ in a cobalt base superalloy. *Mater. Sci. Technol.* **1999**, *15*, 596–598. [CrossRef]
4. Bradley, E.F. *Superalloys: A Technical Guide*; ASM International: Metals Park, OH, USA, 1988.
5. Woulds, M.J.; Cass, T.R. Developments in Mar-M alloy 509. *Cobalt* **1969**, *42*, 3–13.
6. Berthod, P. High temperature properties of several chromium-containing Co-based alloys reinforced by different types of MC carbides (M = Ta, Nb, Hf and/or Zr). *J. Alloys Compd.* **2009**, *481*, 746–754. [CrossRef]
7. Michon, S.; Aranda, L.; Berthod, P.; Steinmetz, P. High temperature evolution of the microstructure of a cast cobalt base superalloy—Consequences on its thermomechanical properties. *Metall. Res. Technol.* **2004**, *101*, 651–662. [CrossRef]
8. Berthod, P. As-Cast microstructures of high entropy alloys designed to be TaC-strengthened. *J. Met. Mater. Res.* **2022**, *5*, 4685. [CrossRef]
9. Berthod, P. Strengthening Against Creep at Elevated Temperature of HEA Alloys of the CoNiFeMnCr Type Using MC-Carbides. In Proceedings of the 152nd TMS Annual Meeting and Exhibition, San Diego, CA, USA, 19—23 March 2023. accepted paper.
10. Berthod, P.; Aranda, L.; Vébert, C.; Michon, S. Experimental and thermodynamic study of the high temperature microstructure of tantalum containing nickel-based alloys. *Calphad* **2004**, *28*, 159–166. [CrossRef]
11. Buchanan, E.R.; Tarshis, L.A. Strengths and failure mechanisms of a cobalt-chromium-tantalum carbide (Co-15Cr-13TaC) directionally solidified eutectic alloy. *Metall. Trans.* **1974**, *5*, 1413–1422. [CrossRef]
12. Thompson, E.R.; Lemkey, F.D. Directionally solidified eutectic superalloys. *Compos. Mater.* **1974**, *4*, 101–157.
13. Karge, L.; Gilles, R.; Mukherji, D.; Beran, P.; Strunz, P.; Hoelzel, M.; Roesler, J. Beyond Ni-base superalloys: Influence of Cr addition on Co-Re base alloys strengthened by nano-sized TaC precipitates. *Phys. B Condens. Matter* **2018**, *551*, 1–5. [CrossRef]
14. Kurz, W.; Fisher, D.J. *Fundamentals of Solidification*; Trans. Tech. Publication: Stafa-Zurich, Switzerland, 1989.
15. Beck, C.G.; Santhanam, A.T. Effect of microstructure on the thermal fatigue resistance of a cast cobalt-base alloy, Mar-M509. *Therm. Fatigue Mater. Compon.* **1976**, *612*, 123–140.
16. Michon, S.; Berthod, P.; Aranda, L.; Rapin, C.; Podor, R.; Steinmetz, P. Application of thermodynamic calculations to study high temperature behavior of TaC-strengthened Co-base superalloys. *Calphad* **2003**, *27*, 289–294. [CrossRef]
17. Lesoult, G. *Traité des Matériaux 5. Thermodynamique des Matériaux: De L'elaboration des Matériaux à la Genèse des Microstructures*; Presses Polytechniques et Universitaires Romandes: Lausanne, Switzerland, 2010.
18. Michel, G.M.; Berthod, P.; Vilasi, M.; Mathieu, S.; Steinmetz, P. Protection of cobalt-based refractory alloys by chromium deposition on surface. Part I: Sub-surface enrichment in chromium by pack-cementation and diffusion. *Surf. Coat. Technol.* **2011**, *205*, 3708–3715. [CrossRef]
19. Michel, G.M.; Berthod, P.; Vilasi, M.; Mathieu, S.; Steinmetz, P. Protection of cobalt-based refractory alloys by chromium deposition on surface. Part II: Behaviour of the coated alloys in oxidation at high temperature. *Surf. Coat. Technol.* **2011**, *205*, 5241–5247. [CrossRef]